

Copper ion beam emission in solid electrolyte $Rb_4Cu_{16}I_{6.5}Cl_{13.5}$

Tushagu Abudouwufu(吐沙姑·阿不都吾甫), Xiangyu Zhang (张翔宇), Wenbin Zuo (左文彬), Jinbao Luo(罗进宝), Yueqiang Lan(兰越强), Canxin Tian (田灿鑫), Changwei Zou(邹长伟), Alexander Tolstoguzov, and Dejun Fu(付德君)

Citation: Chin. Phys. B, 2022, 31 (**4**): 040704. DOI: 10.1088/1674-1056/ac2f31
Journal homepage: http://cpb.iphy.ac.cn; http://iopscience.iop.org/cpb

What follows is a list of articles you may be interested in

Design of a novel correlative reflection electron microscope for *in-situ* real-time chemical analysis

Tian-Long Li(李天龙), Zheng Wei(魏征), and Wei-Shi Wan(万唯实)
Chin. Phys. B, 2021, 30 (**12**): 120702. DOI: 10.1088/1674-1056/ac0522

Response of HD-V2 radiochromic film to argon ions

Lei Cheng(程蕾), Zhe Zhang(张喆), Guiyun Liang(梁贵云), and Yutong Li(李玉同)
Chin. Phys. B, 2021, 30 (**8**): 080702. DOI: 10.1088/1674-1056/ac077f

Structure, conductivity, and ion emission properties of $RbAg_4I_5$ solid electrolyte film prepared by pulsed laser deposition

Jun-Lian Chen(陈军联), Wen-Bin Zuo(左文彬), Xian-Wen Ke(柯贤文), Alexander B Tolstoguzov, Can-Xin Tian(田灿鑫), Neena Devi, Ranjana Jha, Gennady N Panin, De-Jun Fu(付德君)
Chin. Phys. B, 2019, 28 (**6**): 060705. DOI: 10.1088/1674-1056/28/6/060705

Theoretical research on electron beam modulation in a field-emission cold cathode electron gun

Li Xing-Xing, Yuan Xue-Song, Zhang Yu, Yan Yang
Chin. Phys. B, 2014, 23 (**3**): 037901. DOI: 10.1088/1674-1056/23/3/037901

A comparison of the field emission characteristics of vertically aligned graphene sheets grown on different SiC substrates

Chen Lian-Lian, Guo Li-Wei, Liu Yu, Li Zhi-Lin, Huang Jiao, Lu Wei
Chin. Phys. B, 2013, 22 (**10**): 107901. DOI: 10.1088/1674-1056/22/10/107901

Copper ion beam emission in solid electrolyte $Rb_4Cu_{16}I_{6.5}Cl_{13.5}$

Tushagu Abudouwufu(吐沙姑·阿不都吾甫)[1,2,3], Xiangyu Zhang (张翔宇)[1,2], Wenbin Zuo (左文彬)[1,2], Jinbao Luo(罗进宝)[1,2], Yueqiang Lan(兰越强)[1,2], Canxin Tian (田灿鑫)[4], Changwei Zou(邹长伟)[4], Alexander Tolstoguzov[1,5], and Dejun Fu(付德君)[1,2,†]

[1] *Key Laboratory of Artificial Micro and Nanostructures of Ministry of Education and Hubei Key Laboratory of Nuclear Solid Physics, School of Physics and Technology, Wuhan University, Wuhan* 430072, *China*
[2] *Shenzhen Institute of Wuhan University, Shenzhen* 518057, *China*
[3] *Zhuhai Tsinghua University Research Institute Innovation Center, Zhuhai* 519000, *China*
[4] *School of Physics and Technology, Lingnan Normal University, Zhanjiang* 524048, *China*
[5] *Utkin Ryazan State Radio Engineering University, Ryazan* 390005, *Russian Federation*

(Received 2 July 2021; revised manuscript received 9 October 2021; accepted manuscript online 13 October 2021)

Copper ion conducting solid electrolyte $Rb_4Cu_{16}I_{6.5}Cl_{13.5}$ was prepared by means of mechano-chemical method. The structure and morphology of the powder was investigated by x-ray diffraction and scanning electron microscopy. The grain size was estimated to be 0.2–0.9 μm and the ionic conductivity at room temperature was approximately 0.206 S/cm. The solid electrolyte $Rb_4Cu_{16}I_{6.5}Cl_{13.5}$ was exploited for copper ion beam generation. The copper ion emission current of several nA was successfully obtained at acceleration voltages of 15 kV and temperature of 197 °C in vacuum of 2.1×10^{-4} Pa. A good linear correlation between the logarithmic ion current ($\log I$) and the square root of the acceleration voltage ($U_{\rm acc}$) at high voltage range was obtained, suggesting the Schottky emission mechanism in the process of copper ion beam generation.

Keywords: solid electrolyte, mechano-chemical synthesis, ion emission, ion-beam source

PACS: 07.77.Ka, 79.70.+q, 82.45.Gj **DOI:** 10.1088/1674-1056/ac2f31

1. Introduction

Solid electrolytes also called fast ionic conductors are a class of materials exhibiting high ionic conductivity and low activation energy.[1] They have been extensively studied and investigated for broad applications in the fields of energy storage, electrochemical devices, solid-state batteries, and ion beam generation.[2–4] The interest in solid state ionics leads to numerous researches of solid electrolytes. Up to date, researchers have explored ion-conducting materials with various mobile ions, e.g., H^+, Li^+, Na^+, K^+, Ag^+, Cu^+, F^-, and O^{2-}.[5–13] Among them, Ag^+ and Cu^+ ion conducting solid electrolytes attract special attention due to their extremely high ionic conductivity ($\sim 10^{-1}$ S/cm) at room temperature, for example, MAg_4I_5 (with $M = NH_4$, Na, Rb)[14] and Na-β-alumina.[15]

The framework crystalline ion conducting materials are polymorphic systems showing significant differences in ion conductivity between polymorphs. Contrary to solid electrolytes, especially in terms of ion transport or ion emission, liquid electrolytes can be operated neither at high temperatures due to their volatility and thermal instability nor at too low temperatures because of a large increase of their cell impedance.[16] The key point to achieve high conductivity at relatively low temperatures is a stabilization of the ion conductivity. Typical examples of the useful solid electrolyte materials are yttria-stabilized zirconia (YSZ) as oxide ion conductors,[17] tin-doped PbF_2 representing fluoride ion conductors,[18] and KAg_4I_4CN,[19] $(AgI)_{0.5}(AgPO_3)_{0.5}$,[20] $RbAg_4I_5$,[21,22] $CsAg_4Br_{3-x}I_{2+x}$,[23,24] $Rb_4Cu_{16}I_7Cl_{13}$, etc.[25] as silver or copper ion conductors, successfully improving ion conductivity at low temperatures.

It is worth noting that the solid electrolytes containing copper or silver metal have the advantages of space saving and simple structure, which is believed to be useful for fabrication of solid state ion sources. In particular, copper-based solid electrolytes can be deposited with the desired species on substrates without complicated machining processes. Consequently, it is high technological interest to utilize the deposition atoms with easy access. The ionic conductivity of $Rb_4Cu_{16}I_7Cl_{13}$ is reported to reach the highest value at room temperature, among all known solid state electrolytes.[26,27] In space technological area, copper-based solid electrolytes may be used in the form of ion emitter arrays for the field emission electric propulsion, owing to the low operating temperature, long lifetime, small energy spread and small size of the ion source. In this work, $Rb_4Cu_{16}I_{6.5}Cl_{13.5}$ solid electrolyte powders were prepared by ball milling and followed by deposition of $Rb_4Cu_{16}I_{6.5}Cl_{13.5}$ film by thermal evaporation dipping method to cover a tip emitter. The crystal structure and copper ion beam generation of synthetic materials are studied. The relationships of ion beam intensity to working temperature (I–T) and acceleration voltage (I–U) are tested by measuring the beam current.

[†]Corresponding author. E-mail: djfu@whu.edu.cn

© 2022 Chinese Physical Society and IOP Publishing Ltd

2. Experimental details

2.1. Synthesis and characterization of $Rb_4Cu_{16}I_{6.5}Cl_{13.5}$ powders

The mechano-chemical method of ball milling was used to synthesize $Rb_4Cu_{16}I_{6.5}Cl_{13.5}$ powder. The commercially purchased RbCl (Acros organics, 99.8%), CuI (Shanghai Hushi Laboratorial Equipment Co., Ltd, 99.5%) and CuCl (Alfa Aesar, 99%) powder was mixed in molar ratio of 8:13:19. Then, the mixture was placed in an agate container for ball milling process. The container was put in a vacuum sleeve filled with dry argon. The mechanical milling was performed in a planetary ball-milling apparatus (Nanjing, QM-QX2). The rotation rate was 480 rpm.

The crystalline phase composition of the synthesized $Rb_4Cu_{16}I_{6.5}Cl_{13.5}$ samples was identified by powder x-ray diffraction (XRD, Bruker company) using Cu K_α radiation ($\lambda = 0.1542$ nm) over the 2θ range of 10°–50°. The morphology and elemental composition were examined by scanning electron microscopy (SEM, Zeiss Sigma) and energydispersive x-ray spectroscopy (EDS). The $Rb_4Cu_{16}I_{6.5}Cl_{13.5}$ powder was pressed into a pellet with diameter of 7 mm and thickness of 1–2 mm by an electric press machine (DY-30, Tianjin KEQIGAOXIN) that could supply pressure of 4 MPa for 2 min, then silver electrodes were deposited on both sides of the pellet by the method of vacuum evaporation. The pellet was used for AC impedance measurements, which were conducted from 10 Hz to 1 MHz at various temperatures using an impedance meter (6500B, Wayne Kerr).

2.2. Construction of copper-based solid electrolyte ion source

To detect the ion beam extracted from the copper ion source based on the $Rb_4Cu_{16}I_{6.5}Cl_{13.5}$ superionic conductor, an experimental setup was constructed, consisting of an emitter assembly, heating device and ion-beam collector, as presented in Fig. 1(a). The Cu^+ ion emitter was made of copper tip with curvature radius of 10 μm and $Rb_4Cu_{16}I_{6.5}Cl_{13.5}$ coatings deposited on its surface. The dipping method was used for the deposition of $Rb_4Cu_{16}I_{6.5}Cl_{13.5}$ coatings, which was described elsewhere.[23] The power supply provided an anode voltage (50–100 V) and acceleration voltage (0–20 kV). The ion beam current was measured by a pico-ammeter.

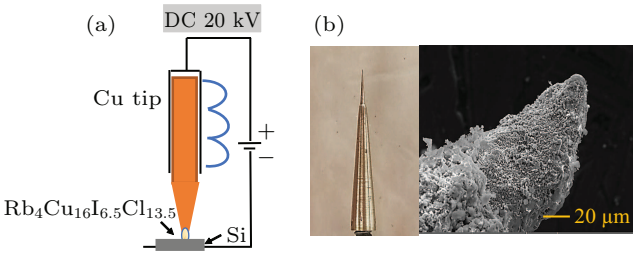


Fig. 1. (a) Schematic illustration of the ion emission test assembly. (b) The photo and SEM image of the copper ion emitter.

3. Results and discussion

3.1. Crystal structure and ion conductivity of $Rb_4Cu_{16}I_{6.5}Cl_{13.5}$

The prepared $Rb_4Cu_{16}I_{6.5}Cl_{13.5}$ powders at different milling times were characterized by x-ray diffraction to identify the phase composition, as shown in Fig. 2. The Rietveld refinement was performed by GSAS software and the goodness-of-fit quantities including the standard R-factors and χ^2 were attached. The right column of Fig. 2 shows the local spectra in the range of 23°–32°, where the characteristic peaks of all phases are located.

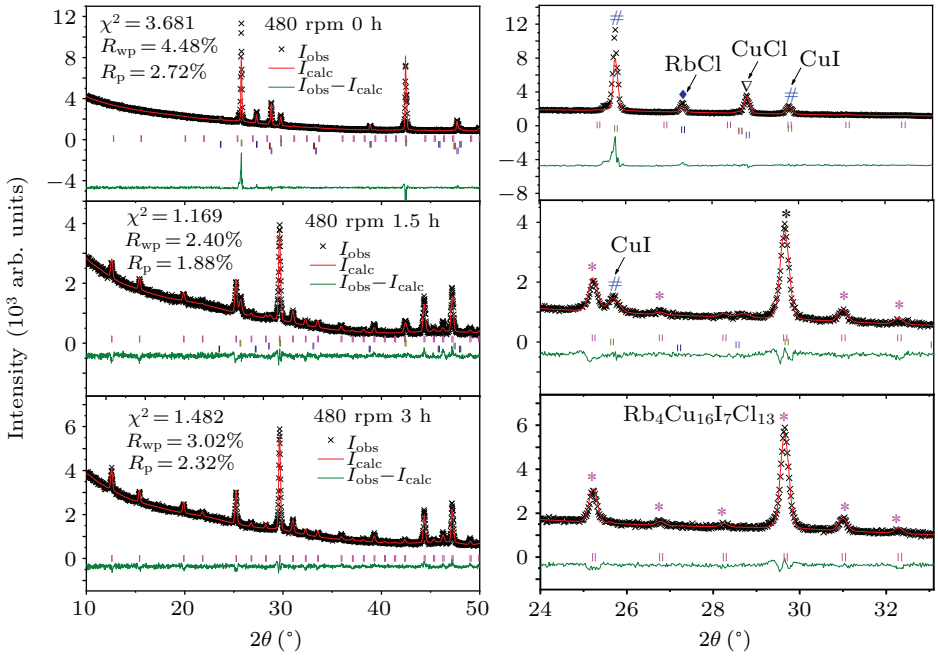


Fig. 2. Rietveld refinement of XRD patterns for synthesized samples at different milling times.

At the beginning of ball milling (480 rpm 0 h), phases of raw materials were identified while the $Rb_4Cu_{16}I_{6.5}Cl_{13.5}$ phase was absent. After 1.5 h of ball milling, the main diffraction peaks were indexed to the high conductive $Rb_4Cu_{16}I_{6.5}Cl_{13.5}$ phase with space group $P4_132$[28] and some CuI impurity phase still remained. When the milling time increased to 3 h, almost pure $Rb_4Cu_{16}I_{6.5}Cl_{13.5}$ phase with good crystallinity was obtained. The crystal structure of $Rb_4Cu_{16}I_{6.5}Cl_{13.5}$ determined by the Rietveld fit is presented in Fig. 3. $Rb_4Cu_{16}I_{6.5}Cl_{13.5}$ has cubic structure, where Rb^+ ions occupy the distorted octahedral sites of Cl^- ions. The Cu^+ ions are predominantly located in Cu1 and Cu2 sites, i.e., 24(e) positions with (0.5148, 0.318, 0.793) and (−0.0071, 0.827, 0.198). A little amount of Cu^+ ions were found to occupy the 8(c) (0.161, 0.161, 0.161) positions (Cu3 sites). Thus, in each unit cell, the 56 sites were only occupied by 16 copper ions, leading to numerous copper vacancies which contributed to the formation of ion-transport pathways. This makes approximately 71% of the sites vacant. It is easily understood that the occupancies of the various Cu^+ sites are essential to diffusion pathways and influence on ionic conductivity.[29] In addition, the copper ion in $Rb_4Cu_{16}I_{6.5}Cl_{13.5}$ can move through faces shared by the $Cu(I/Cl)_4$ tetrahedron to neighboring Cu1, Cu2 and Cu3 sites. From Fig. 3(b) we can find that Cu1 and Cu2 atoms have smaller distances, within 2.392(10)–2.618(10) Å. The Cu1–Cu3 atom range 1.74374(8) Å is a little bit further away, but not a long passage. These tetrahedrons are alternatively sharing faces forming $Cu(I/Cl)_4$ tetrahedrons with each other units and this suggests that the conduction pathway is along with the Cu(1)–Cu(2)–Cu(1) sites.

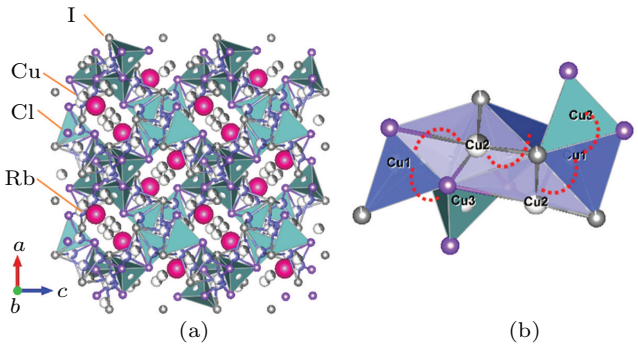


Fig. 3. (a) View of the crystal structure of $Rb_4Cu_{16}I_{6.5}Cl_{13.5}$; (b) Cu1–Cu2 and Cu1–Cu3 ion transport pathway along the nearest atom position.

The ionic conductivity of the pelletized $Rb_4Cu_{16}I_{6.5}Cl_{13.5}$ sample was determined by the alternating current (AC) impedance spectroscopy. Figure 4(a) presents an impedance plot of the copper ion conductor $Rb_4Cu_{16}I_{6.5}Cl_{13.5}$ at room temperature. The impedance values were determined by the intersecting point of the semicircle with the real axis. The ionic conductivity at room temperature was estimated $\sigma \sim 0.206$ S/cm, which is slightly lower than the value of $Rb_4Cu_{16}I_7Cl_{13}$ ($\sigma \sim 0.34$ S/cm) at room temperature. A plot of the calculated Cu^+ ion conductivity as a function of reciprocal temperature is shown in Fig. 4(b). The conductivity versus temperature is fitted well by the Arrhenius equation

$$\sigma = \frac{A}{T}\exp(-E_a/k_BT), \tag{1}$$

where T is the absolute temperature, A is the pre-exponential factor, E_a indicates the activation energy for conduction, and k_B is the Boltzmann constant. The fitting gave the activation energy of the $Rb_4Cu_{16}I_{6.5}Cl_{13.5}$ target to be 0.087(9) eV.

Furthermore, RbCl–CuI–CuCl fast ion conductors use copper ions as the mobile species, and have a highly disordered and distorted structure, which is related to the gradual change in the occupancy of the copper sites. The temperature-dependent conductivity and decomposition potential of $Rb_4Cu_{16}I_7Cl_{13}$ electrolyte is reported to be 0.69 V,[30,31] which is lower than other ion battery materials. For this reason, $Rb_4Cu_{16}I_{6.5}Cl_{13.5}$ ionic conductor has limitations for applications in solid-state batteries.

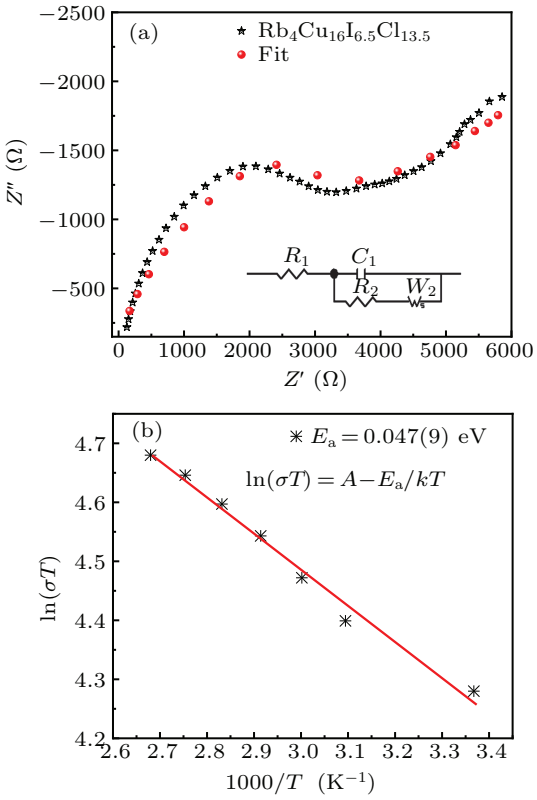


Fig. 4. (a) The ionic conductivity of $Rb_4Cu_{16}I_{6.5}Cl_{13.5}$ sample at room temperature. (b) Arrhenius plot of ionic conductivity as a function of reciprocal temperature.

Figure 5 shows the SEM images of the synthesized samples at different ball milling times. All the prepared samples have the well-defined polyhedron morphology with the particle size of 0.2–0.9 μm, whilst exhibit slight agglomeration. With the increase of milling time, the large particles are broken and the size becomes smaller. When the ball milling extends to 3 h, the fine particles have a small average size and account for the main proportion of the sample.

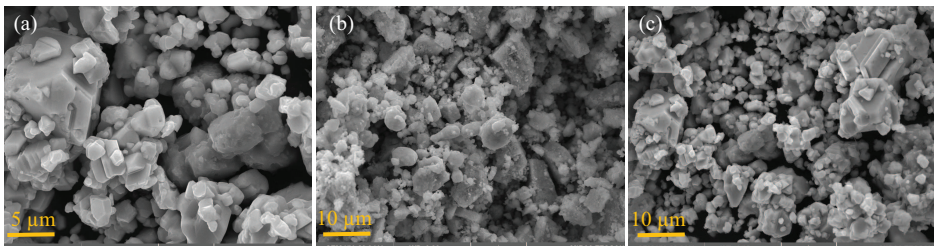


Fig. 5. SEM images of ball milled samples at different times: (a) 0 h, (b) 1.5 h and (c) 3 h.

3.2. Ion beam generation properties

The experimental setup for the Cu^+ ion emission current measurement is shown in Fig. 1(a), which consists of emitter assembly, ion collector and resistive heating device. The photo and SEM image of the copper ion emitter are shown in Fig. 1(b). The curvature radius of the emitter is estimated less than 10 μm. For the ion emission system, the solid electrolyte was not a working substance (propellant) in the usual sense.[32] The mobile ions in solid electrolytes were field-assisted emitted from the cone's apex and the lost ions were replaced (compensated) by the ones in the metal reservoir. Therefore, the metal reservoir played an important role in an effective transmission system in which the movement/replacement of mobile ions was constantly occurring due to the directional mass transfer in the external electric field.

Figure 6 exhibits the current–voltage (I–U) and current–temperature (I–T) characteristics of the copper ion source. The volt-ampere characteristic (I–U) of the SEIS at the working temperature of 197 °C and vacuum of 2.1×10^{-4} Pa is plotted in Figs. 6(a)–6(c). As the acceleration voltage increases, the ion current starts to increase slowly at a threshold voltage of 2 kV, and the current is ∼ 47.5 nA at 15 kV. It can be observed from Fig. 6(d) that the threshold temperature of the ion source was about 180° and was considered as a sign of the ion source activation. For solid electrolyte ion source, a sharp tip was essential for ion emission testing. The curvature radius of the copper tip was estimated to be ∼ 8 μm from SEM image analysis and the sharpness is directly related to the threshold voltage and ion emission current. Although the average current was only 348 pA, Cu^+ ion emission for more than 4 min was observed (Fig. 7), suggesting a continuous Cu^+ supply from the Cu tip during the emission. Based on the Schottky model,[33] the I–U curve satisfied the following equation:

$$\log I \propto \sqrt{U_{\rm acc}}. \tag{2}$$

Thermionic emission is thermally induced flow of charge carriers from a surface. The origin of space charge theory was founded by Child and Langmuir.[34] For the emission current shown in Figs. 6(b) and 6(c), a good linear correlation is achieved in a low voltage range using the space charge limited current model and in a high voltage range using the Schottky model, revealing that the emission of Cu^+ ions from the tip of the solid electrolyte can be expressed by the Schottky-like thermionic emission.

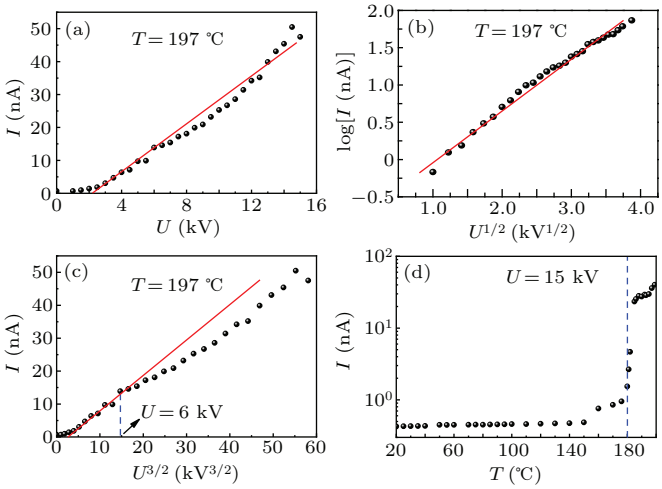


Fig. 6. Characteristics of copper ion emission. I–U characteristics of the ion source at 197 °C based on (a) Ohm's law, (b) Schottky and (c) the space charge limited current model. (d) Temperature dependence of the ion current measured at 15 kV.

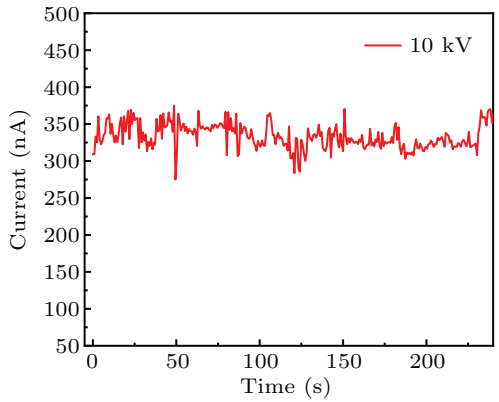


Fig. 7. Running test measured at the working temperature of 197 °C and 10 kV acceleration potential for 4 min.

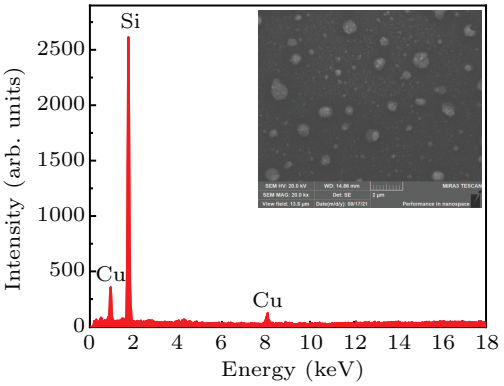


Fig. 8. EDS spectra and the SEM image of the Si wafer irradiated by the emitted ions for a few hours.

To investigate the element composition of the emitted ion beam, a Si wafer was placed at the bottom of Faraday cup as ion collector. EDS spectra and the corresponding SEM image of the Si wafer surface are shown in Fig. 8. The intense signal of Cu element was observed, revealing copper ion emission from the presented ion source. In addition, no other element such as rubidium, chlorine, and iodine were identified in the EDS spectra. Therefore, it could be concluded that almost pure Cu^+ ions were emitted from the source at the sensitivity level of the characterization techniques.

4. Conclusion

In summary, we have investigated the crystal structure and ion emission properties of $Rb_4Cu_{16}I_{6.5}Cl_{13.5}$ solid electrolyte. High ionic conductivity of $Rb_4Cu_{16}I_{6.5}Cl_{13.5}$ is identified in bulk samples. The point-like ion source has been fabricated and tested. The ion beam measurement demonstrates emission of Cu ions from $Rb_4Cu_{16}I_{6.5}Cl_{13.5}$ emitters with ion current in the range of 47.5 nA operated at 197 °C working temperature and 15 kV accelerating voltage. The EDS analysis proves that Cu^+ ion is a dominant component in the emitted ion beam.

Acknowledgements

This work was supported by Shenzhen Municipal Science and Technology Innovation Commission (Grant Nos. JCYJ20170818112901473 and GJHZ20200731095604015) and the Department of Science and Technology of Guangdong Province, China (Grant Nos. 2020A0505100059, 2020A1515011531, and 2020A1515011451). One of the authors (Alexander Tolstoguzov) is grateful to the support of this research by the Ministry of Education and Science of the Russian Federation in the frame of the state assignment (Grant No. FSSN-2020-0003).

References

[1] He S N, Xu Y L, Chen Y J and Ma X N 2020 *J. Mater. Chem. A* **8** 12594
[2] Kanno R, Takeda Y, Imura M and Yamamoto O 1982 *J. Appl. Electrochem.* **12** 681
[3] Gombotz M, Hanghofer I, Eisbacher-Lubensky S and Wilkening H M R 2021 *Solid State Sci.* **118** 106680
[4] Liu H C, Huang J, Cao L X, Su Y, Gao Z Y, Ma P F, Xia S Q, Ge W, Liu Q Y, Zhao S, Wang Y G, Huang J C, Zhou Z H, Zheng P F and Wang C X 2021 *Chin. Phys. B* **30** 086106
[5] Agrawal R C and Gupta R K 1999 *J. Mater. Sci.* **34** 1131
[6] Reuter B and Hardel K 1965 *Z. Anorg. Allg. Chem.* **340** 158
[7] Boolchand P and Bresser W J 2001 *Nature* **410** 1070
[8] Kavun V Y, Gerasimenko A V, Uvarov N F, Polyantsev M M and Zemnukhova L A 2016 *J. Solid State Chem.* **241** 9
[9] Li Q X, Hayashi K, Nishioka M, Kashiwagi H, Hirano M, Torimoto Y, Hosono H and Sadakata M 2002 *Appl. Phys. Lett.* **80** 4259
[10] Creus R, Sarradin J, Astier R, Pradel A and Ribes M 1989 *Mater. Sci. Eng. B* **3** 109
[11] Daiko Y, Yamada T, Yamanishi S, Mineshige A and Yazawa T 2014 *Electrochem.* **82** 901
[12] Daiko Y, Yanagida H, Honda S and Iwamoto Y 2020 *Solid State Ionics* **353** 115400
[13] Yan Z, Pan H Y, Wang J Y, Chen R S, Luo F, Yu X Q and Li H 2020 *Chin. Phys. B* **29** 088201
[14] Owens B B and Argue G R 1967 *Science* **157** 308
[15] Whittingham M S and Huggins R A 1971 *J. Chem. Phys.* **54** 414
[16] Ling S G, Peng J Y, Yang Q, Qiu J L, Lu J Z and Li H 2018 *Chin. Phys. B* **27** 038201
[17] Fujiwara Y, Sakai T, Kaimai A, Yashiro K, Kawada T and Mizusaki J 2006 *J. Vac. Sci. Technol. A* **24** 1818
[18] Berastegui P and Hull S 2002 *Solid State Ionics* **154–155** 605
[19] Mellors G W and Louzos D V 1971 *J. Electrochem. Soc.* **118** 846
[20] Escher C, Thomann S, Andreoli C, Fink H W, Toquant J and Pohl D W 2006 *Appl. Phys. Lett.* **89** 053513
[21] Tolstoguzov A B, Aguas H, Ayouchi R, Belykh S F, Fernandes F, Gololobov G P, Moutinho A M C, Schwarz R, Suvorov D V and Teodoro O M N D 2016 *Vacuum* **131** 252
[22] Chen J L, Zuo W B, Ke X W, Tolstoguzov A B, Tian C X, Devi N, Jha R, Panin G N and Fu D J 2019 *Chin. Phys. B* **28** 060705
[23] Zuo W B, Pelenovich V O, Tolstoguzov A B, Zeng X M, Wang Z G, Song X Q, Gusev S I, Tian C X and Fu D J 2019 *J. Alloys Compd.* **790** 109
[24] Abudouwufu T, Zuo W B, Pelenovich V O, Zhang X Y, Zeng X M, Tolstoguzov A B, Zou C W, Tian C X and Fu D J 2021 *Solid State Ionics* **364** 115634
[25] Takahashi T, Yamamoto O, Yamoda S and Hayashi S 1979 *J. Electrochem. Soc.* **126** 1654
[26] Takahashi T, Kanno R, Takeda Y and Yamamoto O 1981 *Solid State ionics* **34** 283
[27] Masaru A, Haruhito S and Eita H 2021 *Crystals* **11** 1008
[28] Kanno R, Ohno K, Kawamoto Y, Takeda Y, Yamamoto O, Kamiyama T, Asano H, Izumi F and Kondo S 1993 *J. Solid State Chem.* **102** 79
[29] Gao J, Zhao Y S, Shi S Q and Li H 2016 *Chin. Phys. B* **25** 018211
[30] Owens B B 2000 *J. Power Sources* **90** 2
[31] Takehiko T, Osamu Y, Shuji Y and Hoyoshi S 1979 *J. Electrochem. Soc.* **126** 1654
[32] Zuo W B, Pelenovich V O, Tolstogouzov A B, Ieshkin A E, Zeng X M, Wang Z G, Gololobov G, Suvorov D, Liu C S, Fu D J and Hu D H 2019 *Vacuum* **167** 382
[33] Kiziroglou M E, Li X, Zhukov A A, de Groot P A J and de Groot C H 2008 *Solid-State Electron.* **52** 1032
[34] Benilov M S 2009 *Plasma Sources Sci. Technol.* **18** 014005